CHINESE GEOGRAPHICAL SCIENCE
Volume 8, Number 4, pp. 289– 298, 1998
Science Press, Beijing, China

CONTEMPORARY CLIMATIC CHANGE OVER THE QINGHAI-XIZANG PLATEAU AND ITS RESPONSE TO THE GREEN-HOUSE EFFECT①

Liu Xiaodong (刘晓东) Zhang Minfeng (张敏锋)
Lanzhou Institute of Plateau Atmospheric Physics, the Chinese Academy of Sciences, Lanzhou 730000, P. R. China
(Received 13 June 1998)

ABSTRACT: The knowledge of contemporary climatic change over the Qinghai-Xizang (Tibet) Plateau (QXP) has been inadequate for a long time due to lack of enough observational data. In this paper, on the basis of monthly temperature and precipitation data in 1961– 1990 from 48 stations on the QXP, the temperature data are extended backward to 1901 with an empirical orthogonal function (EOF) method, microscopic characteristics of contemporary climatic change over the QXP are analyzed, and the response of the plateau climate to global warming is discussed in combination with atmospheric general circulation model (GCM) outputs. The results show that the plateau climate, as a whole, has been warming since the early part of this century, that the precipitation has generally been increasing during the recent 30 years, and that these climatic trends seem to be related to the enhanced greenhouse effect induced by increasing CO_2 concentration in the atmosphere.

KEY WORDS: Qinghai-Xizang Plateau, contemporary climatic change, greenhouse effect, empirical orthogonal function, atmospheric general circulation, CO_2

I. INTRODUCTION

The global average surface-air temperature of the earth has increased by about 0.5℃ since the mid-19th century (Houghton *et al.*, 1990). The trend of the global warming has been paid close attention to by both scientists and governments because climatic warming may bring about various environmental problems. A great many observational analyses and numerical simulation studies have dealt with contemporary climatic changes over diverse regions up to now. However, investigation on contemporary climatic change over the QXP is still insufficient owing to lack of adequate observational data. The QXP, which covers a quarter of the land area of China and is a region with the highest elevation on the earth (an average elevation of more than

① This work is supported by the National and CAS (the Chinese Academy of Sciences) Tibet Research Project.

4000 m above sea level), has unique plateau climate and important contribution to global climatic change(Ye *et al.*, 1979). By use of observational and extended climatic data and GCM-simulated results, this study presents microscopic characteristics of contemporary climatic change over the QXP and discusses possible influence of the enhanced greenhouse effect induced by increasing CO_2 concentration in the atmosphere on the QXP climatic trend.

II. SPATIAL AND TEMPORAL DISTRIBUTION CHARACTERISTICS OF CONTEMPORARY CLIMATIC CHANGE OVER THE QXP

Most meteorological stations on the QXP were not established until the early 1950s, having had reliable continuous records since the 1960s. Therefore the monthly average data 1961–1990 from 48 stations with nearly continuous records and relatively even distribution were used as an observational dataset of the QXP in this paper. The dataset is more or less inadequate since most of the 48 stations are located in the eastern part and few in the western part of the QXP (Fig. 1b). Quality control of the dataset was performed by replacing few missing or clear-error records of individual stations with values predicted from multiple regression relationships established among a few neighboring and high-correlation stations, thus obtaining continuous monthly surface air temperature and precipitation data from 1961 to 1990.

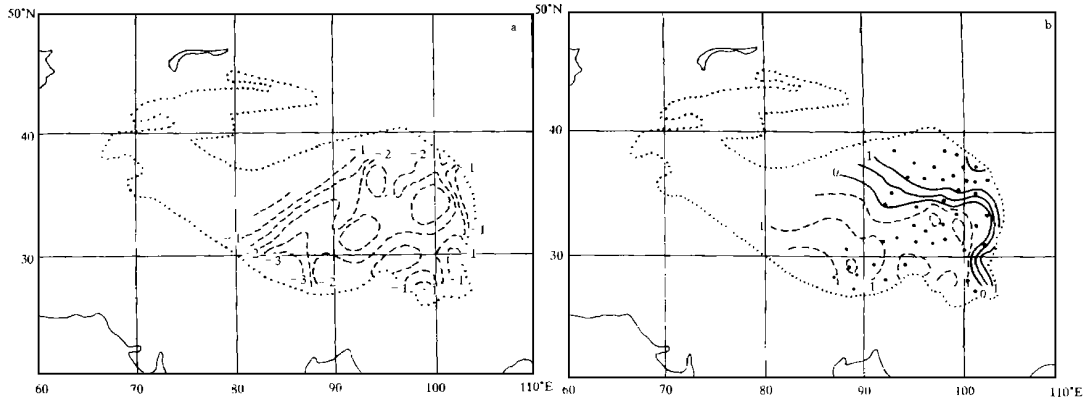

Fig. 1 Spatial structures of the first (a) and second (b) EOF of mean annual surface air temperature anomalies. The contour interval is 0.5℃ and dashed lines indicate negative values. The dot-lines show the outline of the QXP and thick dots denote the positions of 48 meteorological stations used in this study

To know spatial and temporal change of the plateau climate, EOF analyses (Kutzbach, 1967) of mean annual air temperature anomalies and annual precipitation anomaly percentage were completed. The results indicate that variance contribution of the first characteristic vector (CV) of temperature anomaly EOF reaches 50% and accumulative contributions from the first eight CVs explain 91% of the total variance (Table 1). Fig. 1 gives spatial structures of the first and second EOF of mean annual surface air temperature anomalies. Obviously, the first

Table 1 Accumulative variance contributions (AVC) from the first eight EOF characteristic vectors (CV) of annual mean surface air temperature anomalies (%)

CV	1	2	3	4	5	6	7	8
AVC	50	64	76	80	84	87	89	91

CV reflects a consistent variation in air temperature, which is a dominant feature of year-to-year temperature variation over the QXP, while the second CV displays opposite variations between temperatures over the northeastern QXP and those over the southeastern QXP. The consistency in air temperature variation can also be seen from correlations between temperature anomalies of station Qumarleb in the central QXP and those of the 48 stations (Fig. 2). Time coefficients of the first CV practically indicate the variation of the whole plateau temperature field with time. For example, yearly variation of the 48 station average almost quite correspond to that of time coefficients of the first CV (Fig. 3).

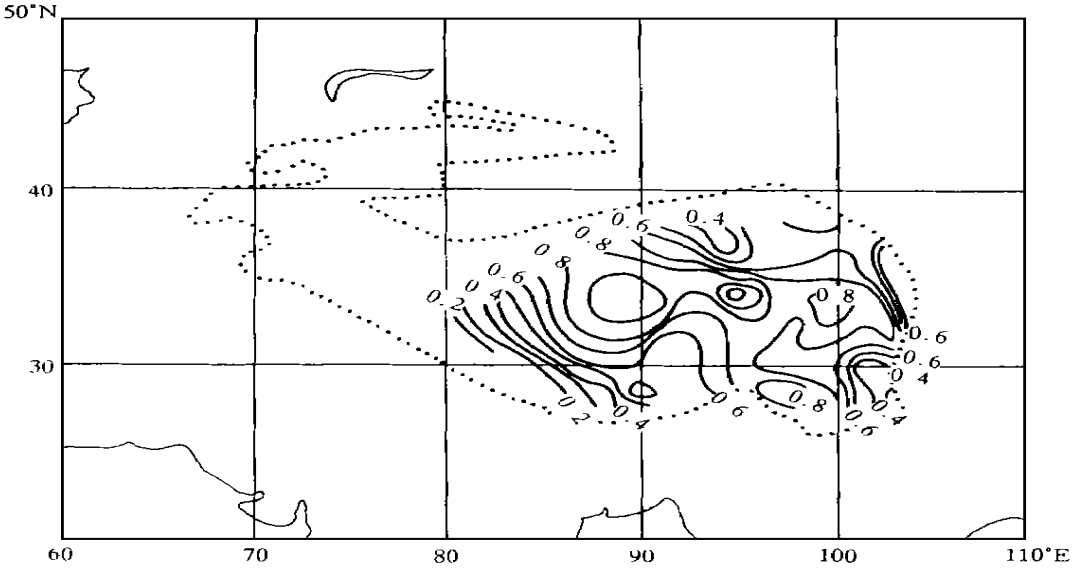

Fig. 2 Distribution of correlation coefficients between mean annual surface air temperature anomalies of Qumarleb station and those of 48 stations on the QXP during the last 30 years. The dot line is the outline of the QXP

The results from EOF analysis of annual precipitation anomalies differ from those for air temperature. The variance contributions of the first CV are 29% and accumulative variance contributions from the first eight CVs 91% (Table 2). In respect to spatial distribution, the first and second CVs show opposite variations in precipitation between the northern and southern QXP (not shown). The third CV presents consistent precipitation variation from the central to northeastern QXP while the fourth CV between the southwestern to northeastern QXP. Knowing these spatial and temporal characteristics of air temperature and precipitation is useful for us to further analyze their changes on a longer time scale.

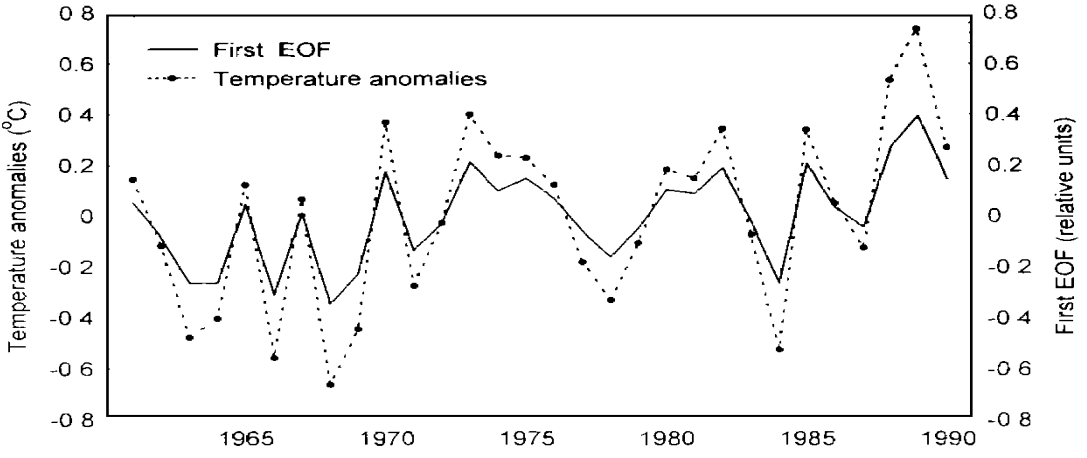

Fig. 3 Yearly variation of mean annual air temperature anomalies of 48 plateau station average and temporal evolution (multiplied by - 1) of their first EOF during 1961- 1990

Table 2 Accumulative variance contributions from the first eight EOF characteristic vectors of annual precipitation anomalies

CV	1	2	3	4	5	6	7	8
AVC	29	42	53	63	69	74	78	81

The above surface-air temperature sequence should be extended as a data sequence of 30 years is not enough to detect climatic trend. Owing to the fact that the temperature field over the QXP is a part of global temperature field and so has certain relations with temperature fields of other parts in the world, a temperature sequence of the QXP on a longer time scale can be obtained by means of an EOF expansion method (Tu, 1986) using some longer observational records in mid-latitudes in the Northern Hemisphere. The method is described briefly as follows.

As has been pointed out before in the EOF analysis of annual mean surface-air temperatures of the 48 stations on the QXP for 30 years, accumulative variance contributions from the first eight CVs account for 91%. Hence the first eight CVs and their time coefficients should have a considerably precise fitting to the original field. Supposing $B^{(1)}_{30\times 48}$, $V_{8\times 48}$ and $Y^{(1)}_{30\times 8}$ denote matrixes of the temperature field consisting of data from the 48 stations during 1961-1990, the first eight CVs and time coefficients, respectively, then

$$B^{(1)}_{30\times 48} = Y^{(1)}_{30\times 8} V_{8\times 48} \quad (1)$$

Table 3 lists correlation coefficients between the temperature field fitted with the first eight CVs and the original temperature field. It can be seen that the correlation coefficient of 30 years average is 0.9, each year having high correlation. Arbitrarily taking Tingri station in the southwestern QXP and Golmud station in the northeastern QXP for examples, results of their fittings are considerably satisfactory (Fig. 4).

Table 3 Correlation coefficients of yearly air temperature field and its fitting with the first eight EOF characteristic vectors

Year	1	2	3	4	5	6	7	8	9	10
1960	0.91	0.90	0.91	0.96	0.93	0.97	0.93	0.91	0.90	0.85
1970	0.85	0.94	0.78	0.81	0.92	0.83	0.87	0.93	0.90	0.83
1980	0.92	0.92	0.86	0.84	0.97	0.99	0.86	0.91	0.89	0.92

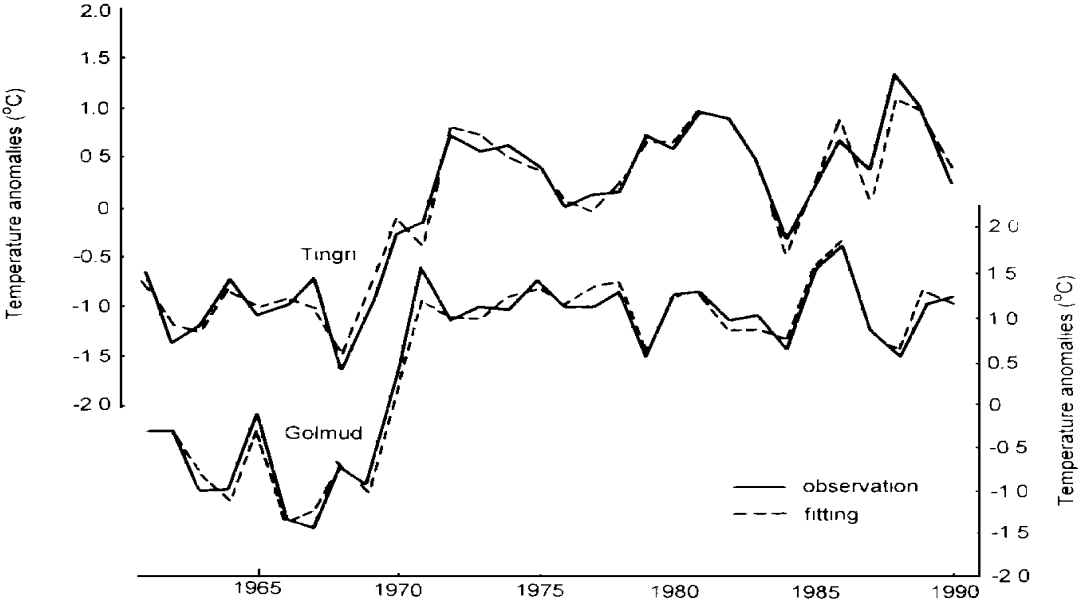

Fig. 4 Yearly air temperature anomalies (solid lines) and their fitting values (dashed lines) with the first eight EOF components for stations Tingri and Golmud

Using a monthly surface-air temperature anomaly dataset on a 5° latitude by 10° longitude global grid (Jones *et al.*, 1992), data from 59 grids having continuous records during 1901–1990, located mainly in mid-latitudes of Europe and North America, was extracted, treated into yearly anomalies and then used for EOF expansion. The results show that the first ten CVs, with accumulative variance contributions of 88%, can reveal principal characteristics of the temperature field consisting of the 59 grids. Matrixes of the temperature field, its first ten CVs and time coefficients during 1901–1990 are denoted as $A_{90\times 59}$, $U_{10\times 59}$ and $X_{90\times 10}$, then

$$A_{90\times 59} = X_{90\times 10}\ U_{10\times 59} \tag{2}$$

On basis of 1961–1990 data of $B^{(1)}_{30\times 48}$ and $A_{90\times 59}$, a regression relationship between time coefficients of their EOF expansions are established

$$Y^{(1)}_{30\times 8} = X^{(1)}_{30\times 10}\ C_{10\times 8} \tag{3}$$

where $X^{(1)}_{30\times 10}$, a sub-matrix of $X_{90\times 10}$, is composed of data of the last 30 years, $C_{10\times 8}$ is the coefficient matrix calculated by linear regression. We assume that the above relation is suitable

out of the 30 years, that is, the relation between the temperature field over the QXP and that over the Northern Hemisphere is the same in the first 60 years as in the last 30 years during 1901– 1990. Consequently, time coefficients of the first 60 years corresponding to matrix $B^{(1)}_{30\times 48}$ of the QXP can be obtained from the time coefficient matrix $X^{(2)}_{60\times 10}$, a sub-matrix of $X_{90\times 10}$ of the Northern Hemisphere for the first 60 years

$$Y^{(2)}_{60\times 8} = X^{(2)}_{60\times 10}\ C_{10\times 8} \qquad (4)$$

In the end by compounding spatial and temporal components through a relation like formula (1), yearly temperature anomaly field during 1901– 1960 will be acquired.

To check the reliability of the extended data simply, we compared five-point Gauss filtered results of mean annual air temperature anomalies for the average of 48 stations over the QXP with mean tree ring indices over the Qilian Mountain in the northeastern QXP(Kang, 1992). It is found that there is a significant correlation, with a correlation coefficient of 0.38 for 80 years in which both of the data are available, exceeding 99% confidence level (Fig. 5). It is thus clear that the extended temperature sequence is believable in displaying the contemporary climatic change over the QXP.

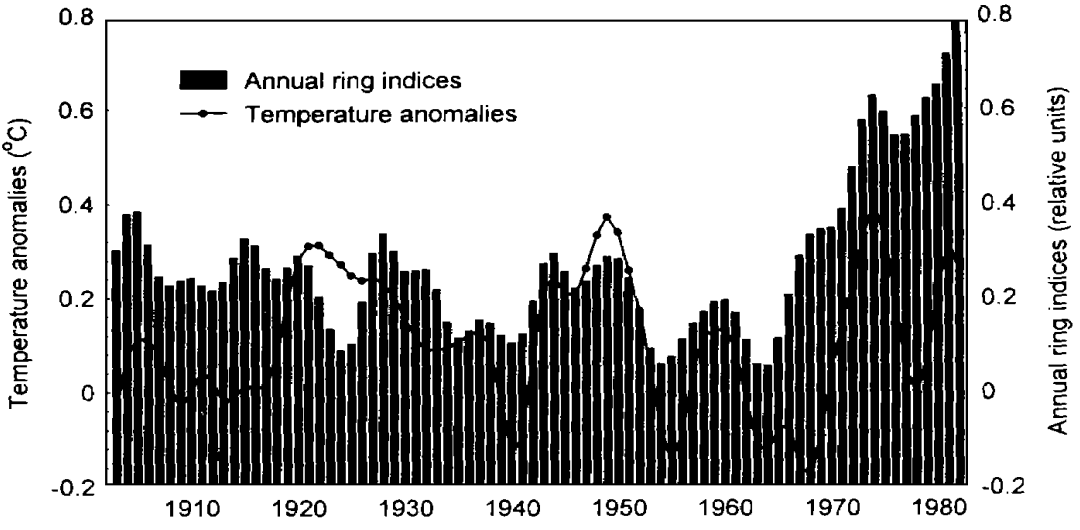

Fig. 5 Five-point Gauss filtered annual mean air temperature anomalies of the QXP and mean tree ring indices over the Qilian Mountain from 1903 to 1982

III. THE RESPONSE OF THE QXP CLIMATIC CHANGE TREND TO GLOBAL WARMING

In order to be compared with the Northern Hemispheric temperature anomalies sequence (Jones *et al.*, 1992), which is relative to 1951– 1970 reference period, the QXP yearly temperature anomalies relative to the same reference period were computed from the above extended data of 90 years. Thereupon 5-year running averages of the two temperature sequences and

their fittings with five order polynomials are plotted in Fig. 6. For the Northern Hemispheric average, there is a trend of warming beginning in the 1920s, reaching a peak in the 1940s, then a trend of cooling until the early 1970s and an other abrupt warming from the 1980s. The general warming trend since the early period of this century and two warming processes also appear over the QXP. It is noteworthy that the mean temperature of the QXP seems to vary ahead of that of the Northern Hemisphere on a time scale of a few decades. The QXP climatic change will be of great interest in global change study if this phenomenon is true. However, these results from the extended data need to be clarified further due to the limitation of the original observational data length.

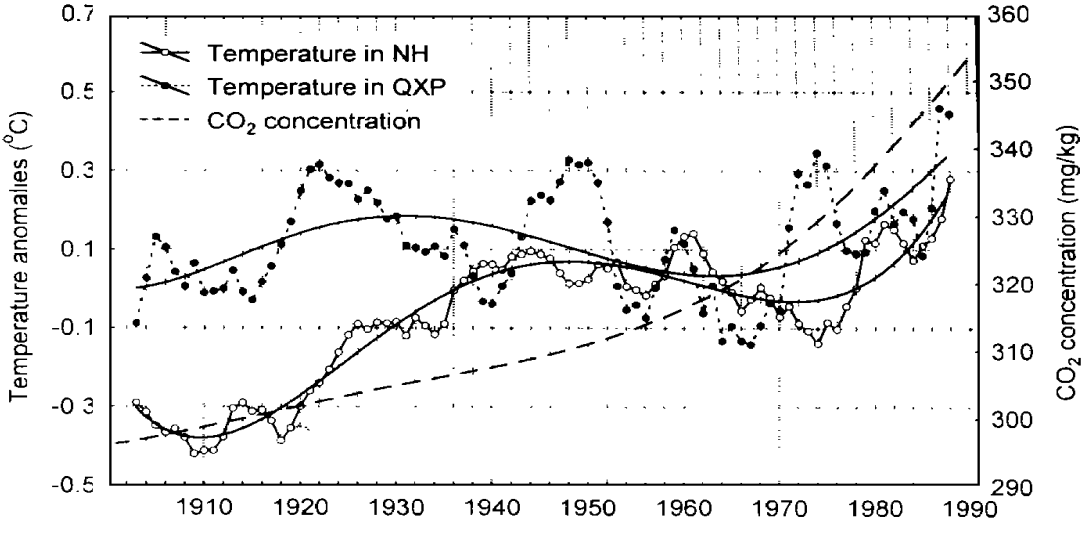

Fig. 6 5-year running mean of average air temperature anomalies over the QXP (solid dot linked line) and the Northern Hemisphere (hollow dot linked line). The solid lines are their fitting curves with five order polynomials; the dashed line shows CO_2 concentration in the atmosphere

Precipitation change of only recent 30 years for the QXP was analyzed. From statistics of ratio of monthly numbers of the QXP stations with positive precipitation anomalies to total number of the stations (48), the ratio is in step with monthly air temperature anomaly of the Northern Hemisphere(Boden *et al.*, 1994) (Fig. 7), which means that the number of stations with more than normal precipitation increases with global warming. In other words, global warming generally helps in increasing the QXP precipitation. However, this result can not illustrate a precipitation trend for a long time because it comes from data of only 30 years. Meanwhile, as the used stations are mainly located in the eastern QXP, it is open to question whether the above result presents a state of the whole QXP.

Many investigators have ascribed global warming since the beginning of industrial revolution to increase in greenhouse gases induced by human activities (Houghton *et al.*, 1990). In

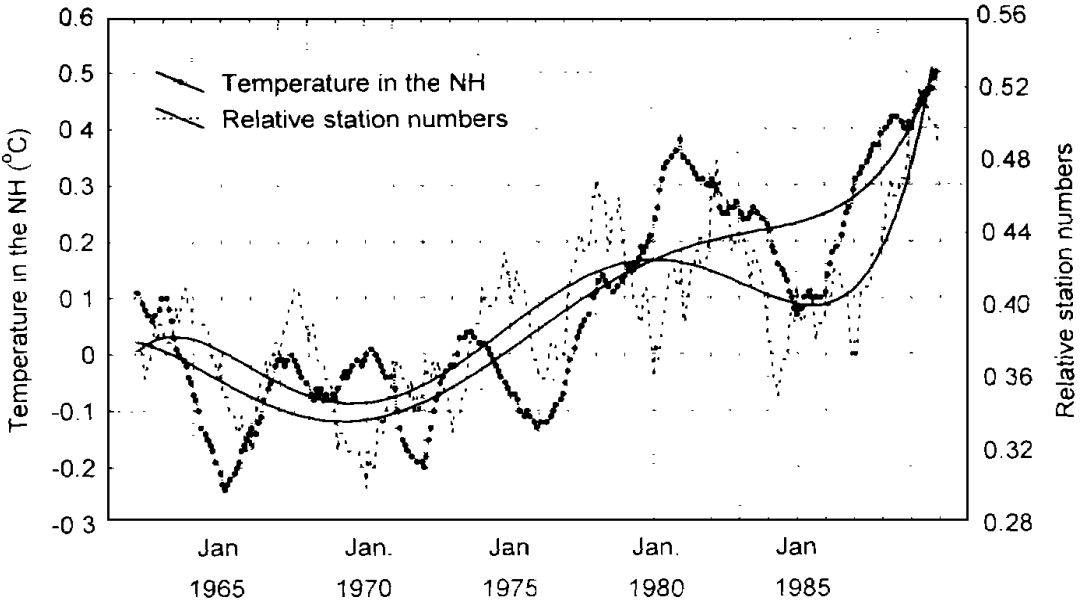

Fig. 7 13-month running mean of monthly relative numbers of the QXP stations with positive precipitation anomalies and monthly air temperature anomalies over the Northern Hemisphere. The solid lines are their fitting curves with five order polynomials

Fig. 6 we depict spline-interpolated yearly atmospheric CO_2 concentration (Enting *et al.*, 1994), observed at Mauna Lao Observatory, Hawaii and in the Vostok ice core in Antarctica. It appears that the climatic warming over the QXP is related to CO_2 increase, especially since the 1970s, though the increase of CO_2 concentration can not be used to explain the cooling in the 1960s.

To explore possible influence of increase in atmospheric CO_2 concentration on the QXP climatic change, outputs of two 100-year integrations with the Geophysical Fluid Dynamics Laboratory (GFDL) ocean-atmosphere coupled model, one of which is a transient change experiment with 1% increase in the atmospheric CO_2 concentration per year and the other control experiment (Manabe *et al.*, 1991), were analyzed. The results show that the climate over the QXP more than 2000 meters above sea level, covering total 16 model grids, tends to be warming and wetting, having the same tendency as the global average but a greater range than the global average (Fig. 8).

As has been found in similar experiments with other GCMs, the warming magnitude in high-latitudes is greater than in middle and low latitudes in the Northern Hemisphere. With respect to mid-latitudes (20°–60°N), it is found that the warming for the QXP is much stronger than that for the land average in the same latitude belt (Fig. 9). The climate over sea changes very slow, even having a slight cooling, which has been believed related to weakening of temperature-salinity circulation in ocean (Manabe *et al.*, 1991). It seems that contemporary climatic warming is a response of atmosphere to increase in greenhouse gases. Moreover, the QXP

is an area having strong response.

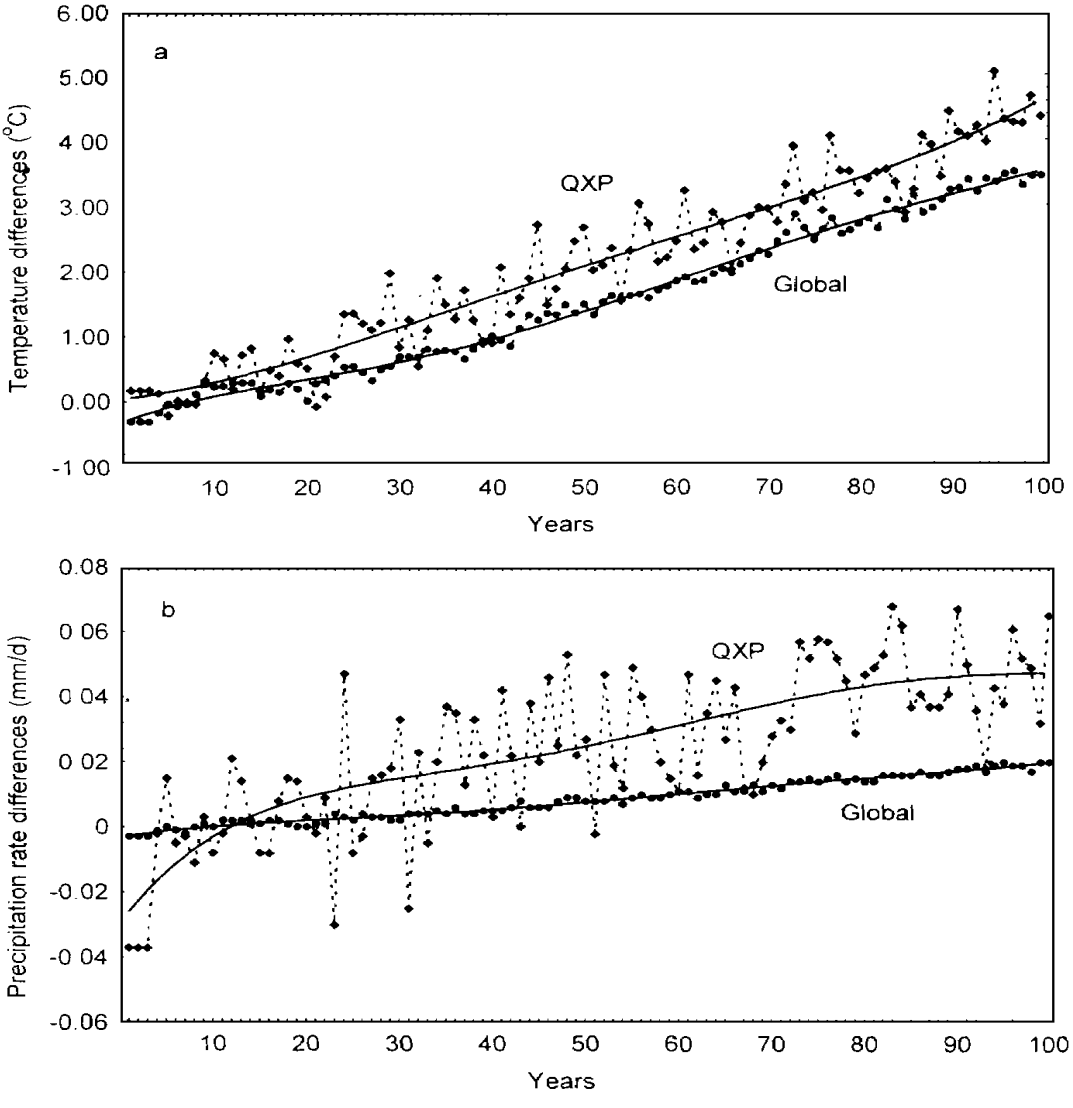

Fig. 8 Differences in air temperature (a) and in precipitation rate (b) over the QXP and on the global scale between two 100-year integrations of atmospheric CO_2 transient change experiment and control experiment with GFDL ocean-atmosphere coupled model

IV. CONCLUSION

The surface-air temperature has generally been ascending since early this century and precipitation increasing during the recent 30 years over the QXP. Trends of the temperature and precipitation seem to be related to the enhanced greenhouse effect induced by increasing CO_2 concentration in the atmosphere. Although many factors except greenhouse gases impact climatic change, the climatic warming trend over the QXP should be paid enough attention to a-

long with continuous increase in concentration of greenhouse gases produced by human activities in the future.

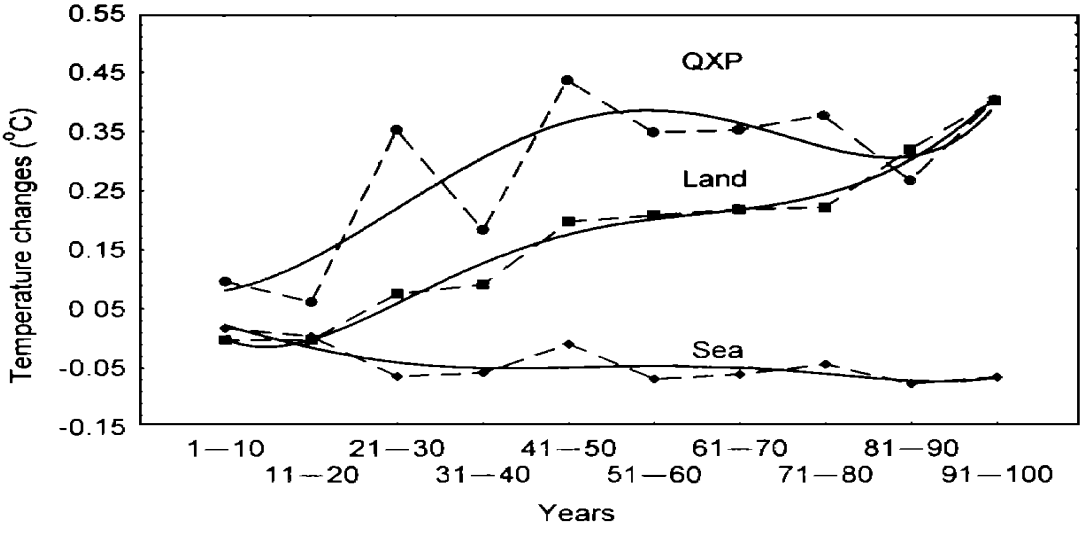

Fig. 9 Surface-air temperature changes induced by atmospheric CO_2 increase over the QXP, the land and sea in 20°– 60°N in 100-year integrations of GFDL GCM

REFERENCES

Boden T. A., D. P. Kaiser, R. J. Sepanski, F. W. Stoss (Eds.), 1994. *Trends' 93: A Compendium of Data on Global Change*. CDIAC, Oak Ridge National Laboratory, 622– 623.

Enting I. G., T. M. L. Wigley, M. Heimann (Eds.), 1994. *Future Emissions and Concentrations of Carbon Dioxide: Key Ocean/Atmosphere/Land Analyses*. Commonwealth Scientific and Industrial Research Organization, Aspendale, Australia, CSIRO Division of Atmospheric Research Technical Paper No. 31.

Houghton J. T., G. J. Jenkins J. J. Ephraums, 1990. *Climate Change: The IPCC Scientific Assessment*. Cambridge: Cambridge University Press, 1– 365.

Jones P. D., K. R. Briffa, 1992. Global surface air temperature variations over the twentieth century: Part 1, Spatial, temporal and seasonal details. *Holocene*, 2: 105– 179.

Kang Xingcheng, 1992. An exploration of historical climatic change over Qilian mountain. *Special Research Issue of Lanzhou Institute of Glaciology and Geocryology, Chinese Academy of Sciences*, No. 7. Beijing: Science Press, 54– 63. (in Chinese)

Kutzbach J. E., 1967. Numerical eigenvectors of sea– level pressure, surface temperature and precipitation complexes over North America. *J. Appl. Meteor.*, 16: 791– 802.

Manabe S., R. J. Stouffer, M. J. Spelman *et al.*, 1991. Transient response of a coupled ocean-atmosphere model to gradual changes of atmospheric CO_2. Part I: Annual mean response. *J. Climate*, 4: 785– 818.

Tu Qipu, 1986. A method of extending an time series sequence of air temperature. *J. Nanjing Institute Meteor.*, 9: 19– 30. (in Chinese)

Ye Duzheng, Gao Youxi, 1979. *The Meteorology of the Qinghai-Xizang (Tibet) Plateau*. Beijing: Science Press, 1– 278. (in Chinese)